

THEORY OF CHEMICAL REACTION DYNAMICS

Edited by:

ANTONIO LAGANA
Department of Chemistry
University of Perugia
Perugia, Italy

and

GYÖRGY LENDVAY
Institute of Chemistry
Chemical Research Center
Budapest, Hungary

Kluwer Academic/Plenum Publishers
New York/Boston/Dordrecht/London/Moscow

PREFACE

Theoretical treatment of the dynamics of chemical reactions has undergone a spectacular development during the last few years, prompted by the progress in experiments. Beam production, spectroscopic detection using high resolution, polarized lasers allowing energy and angular momentum selection, etc. have advanced so much that the experiments now offer detailed scattering information for theory to explain and rationalize. At the same time advances in computing and networking technologies for heterogeneous and grid environments are giving new possibilities for theoretical studies of chemical reactivity. As a consequence, by now calculation of atom+diatom reactions has become routine, accurate methods have been developed to describe reactions in tetraatomic systems, non-adiabatic reactions are being studied in simultaneous experimental and theoretical efforts, and statistical theories of unimolecular reaction dynamics are applied to systems that were a mystery a few years ago.

The increased interest in the field is testified by an intense activity of conferences, schools and collaborative networks. The NATO scientific division has traditionally contributed to this field through supporting workshops and schools. Along this line we organized the NATO Advanced Research Workshop on the Theory of the Dynamics of Chemical Reactions in Balatonföldvár, Hungary in June, 2003. The workshop has given a snapshot of the current status of research in reaction dynamics. At the meeting 36 papers were given, with enlightening discussions. Accurate time-dependent and time-independent methods of quantum scattering, treatment of non-adiabatic processes, studies of associative and inelastic collisions, calculation of potential surfaces received increased attention.

This book summarizes the proceedings of the Workshop, and is dedicated to Professor E.E. Nikitin on the occasion of his 70th birthday. The authors of 21 papers of the meeting agreed to make a written contribution aimed at giving a review of their recent work instead of just summarizing the brand new results, with the hope of providing researchers in the field with a useful reference.

We thank all the authors for their helpful collaboration. The grant from the NATO Science Program, without which the meeting could not have been organized, is gratefully acknowledged, as well as support from the Hungarian Ministry of Education. We thank Dr. Ákos Bencsura, Erika Bene and Tamás

Vértesi for their participation in organizing the meeting. The efficient help of Dr. Andrea Hamza in editing the book is highly appreciated.

Antonio Laganà
Department of Chemistry,
University of Perugia, Italy

György Lendvay
Institute of Chemistry,
Hungarian Academy of Sciences
Budapest, Hungary

CONTENTS

Dedication to Evgueni Nikitin	1
Anatoli I.Maergoiz, Evgueni E.Nikitin, Jürgen Troe and Vladimir G.Ushakov: Asymptotic interactions between open shell partners in low temperature complex formation: the $\text{H}(\text{X}^2\text{S}_{1/2})+\text{O}_2(\text{X}^3\Sigma_g^-)$ and $\text{O}({}^3\text{P}_{j\sigma})+\text{OH}(\text{X}^2\Pi)$ systems	21
Millard H. Alexander, Yi-Ren Tzeng and Dimitris Skouteris: Differential cross sections for abstraction reactions of halogen atoms with molecular hydrogen including nonadiabatic effects	45
Gábor Halász, Ágnes Vibók, Alexander M. Mebel and Michael Baer: On the quantization of the electronic non-adiabatic coupling terms: The $\text{H}+\text{H}_2$ system as a case study	67
Biswajit Maiti and George C. Schatz: Non-adiabatic dynamics in the $\text{O}+\text{H}_2$ reaction: a time- independent quantum mechanical study	89
Vladimir I. Osherov, Vladimir G. Ushakov and Hideki Nakamura: Nonadiabatic transitions between asymptotically degenerate states	105
Boris M.Smirnov: Coupling of electron momenta in ion-atom collisions	129
Gabriel G. Balint-Kurti and Alex Brown: Time-dependent wavepacket calculations for reactive scattering and photodissociation	149
Pascal Honvault and Jean-Michel Launay: Quantum dynamics of insertion reactions	187
Hua Guo: Chebyshev propagation and applications to scattering problems	217
John C. Light and Hee-Seung Lee: Molecular dynamics: energy selected bases	231
Vincenzo Aquilanti, Fernando Pirani, David Cappelletti, Franco Vecchiocattivi and Toshio Kasai: Molecular reaction stereodynamics: in search of paths to overcome steric hindrances to reactivity	243
Gunnar Nyman: The rotating bond umbrella model applied to atom-methane reactions	253

MANIPULATION OF ATOMS AND MOLECULES WITH LASER RADIATION AND EXTERNAL FIELDS

MARCIS AUZINSH

*Department of Physics, University of Latvia, 19 Rainis boulevard,
Riga, LV-1586, Latvia, mauzins@latnet.lv*

Abstract. The paper provides analysis of a process, when a laser radiation absorption of a specific polarization creates a specific spatial distribution of molecular bonds and angular momenta of small molecules. It is discussed how an external fields – electric or magnetic – can influence this distribution. Some practical examples involving optical polarization of molecules in magnetic and electric fields are presented.¹

1. Introduction

Laser radiation has proved to be an efficient tool to control the shape of wave functions. The ability to control the shape of a quantum state may lead to methods for bond-selective chemistry and novel quantum technologies such as quantum computing. The classical coherence of laser light has been used to guide quantum systems into desired target states through interfering pathways. These experiments allow to control properties of the target state such as light absorption, fluorescence, angular momentum or molecular bond spatial orientation etc.

Probably coherent effects in atomic excitation with light were studied first by Wilhelm Hanle. The very first publication about the effect, which is now called Hanle effect, appeared in *Zeitschrift für Physik* as early as in 1924 [1]. In the paper it was shown that the resonance fluorescence of Hg excited with linear polarized light is depolarized by an external magnetic field. That publication does

¹I have a privilege to know Prof. Evgueni Nikitin for many years. For the first time as a young student I met him at a conference in the former Soviet Union at which optical polarization of atoms and molecules was discussed. Later on our ways crossed several times and I had an opportunity to work with Prof. Nikitin on several projects and to admire his scientific intuition, deep knowledge and skills in application of advanced mathematical techniques to solve problems in physics elegantly. I feel very delighted and honored to dedicate this paper to Prof. Evgueni Nikitin on the occasion of his seventieth birthday.

not provide solely the measurements of this depolarization. It also shows that the plane of polarization of the fluorescence is rotated by the external magnetic field. To analyze this effect W. Hanle used a model of decaying linear oscillators that precess in the magnetic field with an angular velocity depending on the magnetic field strength. In this first paper the quantum theoretical importance of the effect was already discussed.

During the following years, efforts to provide a consistent interpretation of the effect played an important role in the development of quantum theory. The essence of Hanle effect, as we understand it today, is the creation of low frequency coherences between magnetic Zeeman sublevels of an atomic state and the destruction of these coherences by lifting of the magnetic sublevel degeneracy by an applied external magnetic field. These Zeeman coherences are associated with spatial polarization (orientation or alignment) of angular momenta of atoms or molecules. To this day Hanle effect still is an effective tool to study atomic [2] and molecular structure [3].

If the optical field that excites atoms or molecules is strong enough, it can create Zeeman coherences not only in the excited state of atoms or molecules, but also in the ground state. In a slightly different context this effect for the first time was studied as an optical pumping of atomic states.

As early as in 1949 Kastler [4] draws attention to the remarkable properties of the interaction of resonance light with atoms. Kastler points out that the absorption and scattering of resonance light could lead to large population imbalances along with atomic excited state also in atomic ground state. Ground state optical pumping soon was observed experimentally by Brossel, Kastler and Winter [5] and by Hawkins and Dicke [6].

In the absence of the external fields, the effect of optical pumping can easily be analyzed without using the concept of atomic coherences, but if one is willing to consider the influence of the external fields on optically pumped atoms or molecules then the idea about Zeeman coherences in the ground state of atoms or molecules becomes vital. In this case, we are speaking about creation of dark states or coherent population trapping. This effect was first directly observed in 1976 in the interaction of sodium atoms with a laser field [7]. In the case of coherent population trapping the destructive quantum interference between different excitation pathways causes the trapping of population in a coherent superposition of ground state sublevels. Once established, such a superposition (a dark state) [8] is immune against further radiative interaction. As a result, a fluorescence from an ensemble of atoms decreases, while the intensity of the transmitted light increases. An external magnetic field \mathbf{B} applied perpendicularly to the light polarization vector \mathbf{E} destroys the coherence between ground state sublevels and restores the absorption and fluorescence of the ensemble of atoms.

To describe all phenomena related to the creation and evolution of coherences created in an ensemble of atoms or molecules, one can deal with probability amplitudes for different quantum states involved in the process of light — matter

interaction. Nevertheless, it is a rather complicated business to follow all the amplitudes and, what is most important, all the phase relations between the states involved in the process. It is much more convenient to describe an ensemble of particles by means of quantum density matrix. The application of quantum density matrix for the description of atomic processes was pioneered by U. Fano (see, for example [9]). Currently this approach is recognized as very fruitful and is used in various contexts. In a standard form the interaction of laser radiation with gaseous atoms or molecules is described by means of the Liouville or optical Bloch equation for the quantum density matrix [8]. In the case of optical Bloch equations the use of monochromatic, intense optical field is assumed.

At the same time very often the real optical field interacting with atoms has rather broad spectral profile, width of which is broader or comparable with the inhomogeneous width of the atomic transition. In this case, a broad spectral line approximation for quantum density matrix approach has proved to be very rewarding. This approximation was introduced in the 1960s by C. Cohen-Tannoudji for excitation of atoms with ordinary light sources [10]. This was an era before lasers. Later on it was adjusted for application for excitation of atoms with multimode lasers [11] and for excitation of molecules in the case of large angular momentum states [3, 12].

It is demonstrated in different occasions that the quantum density matrix solutions for atomic or molecular states can be connected to a form of created wave function and spatial distribution of atomic angular momentum [13, 14]. This approach proved to be especially fruitful in the case of molecules. For example, for diatomic molecules that typically possess states with very large angular momentum quantum numbers $J \propto 100$, the spatial orientation of this angular momentum with respect to a chosen direction of quantization axis varies almost continuously. As a result, the transition from the quantum density matrix solution to the spatial distribution of angular momentum and molecular axes seems to allow to have a very clear insight into the processes taking place during the interaction of molecular ensemble with the optical fields [3, 15]. This method allows one to prepare molecules in a desired state of their orientation in a laboratory frame as well. It also allows one to study different stereoscopic or spatial effects of molecular interactions and interaction of molecule with the laser radiation.

2. Angular momentum polarization by laser radiation

2.1. VECTOR MODEL

The main purpose of this vector model treatment of light absorption in molecules is to provide a simple visual model for the absorption of light by diatomic molecules in which the geometrical implications of light polarization and molecular spatial orientation may be made apparent.

Let us start with the following picture of laser light interacting with diatomic molecule. We have a rotating diatomic molecule with a large total angular momen-

tum J . It is largely created by molecular rotation, which contributes an angular momentum N as a main part of J . Additionally, it is created also from an electronic angular momentum L , and, more precisely, from its projection Λ on an internuclear axis of the molecule. Due to the axial symmetry of the internal fields in the molecule this is a quantity, which is conserved in a molecular frame (see Fig. 1).

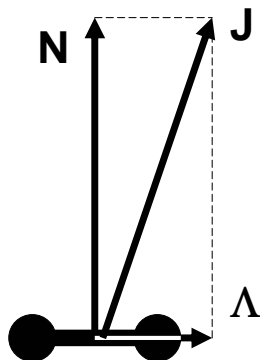


Figure 1. The main angular momentum components in a diatomic molecule.

If we ask a simple question – what is changing, if such a molecule absorbs radiation in an electronic transition? The answer is obvious. Light can change an electron motion in the molecule and it means that electronic angular momentum in molecule and along with it the projection of this angular momentum on internuclear axis will be changed. In molecular spectroscopy one can distinguish two different types of transitions between electronic states of diatomic molecule. One is a perpendicular transition in which Λ is changed by ± 1 and another one is a parallel transition when Λ remains constant. For example $\Sigma \longleftrightarrow \Sigma$ or $\Pi \longleftrightarrow \Pi$ are parallel molecular transitions, but $\Sigma \longleftrightarrow \Pi$ is a perpendicular transition. The notation of the transition as being parallel or perpendicular is coming from the vector model and an analysis of the behavior of transition dipole moment during the transition in this model. For the parallel transition this dipole moment oscillates along the internuclear axis, while in the case of perpendicular transition it rotates in a plane perpendicular to the internuclear axis. It is obvious, how this behavior of the transition dipole moment is coming into existence. If, for example, we have a $\Sigma \rightarrow \Pi$ absorption, then as a part of the transition probability we will need to calculate a dipole transition matrix element

$$\langle J' \Lambda = 1 | \hat{d} | J'' \Lambda = 0 \rangle, \quad (1)$$

where \hat{d} denotes transition dipole operator and J' and J'' denote the angular momentum quantum numbers of an excited and ground state respectively. As we see,

during this transition projection of an angular momentum J on the internuclear axis is increased by 1. This can be provided only by the dipole moment component d_{mol}^{+1} which in an angular momentum vector model can be associated with a rotation of the transition dipole momentum in a counterclockwise direction in a plane perpendicular to the quantization axis with a frequency ω [13], in this particular case – internuclear axis (see Fig. 2 *a*). In a similar way the behavior of the transition dipole momentum of molecule during the parallel type of transition, for example $\Sigma \longleftrightarrow \Sigma$ transition

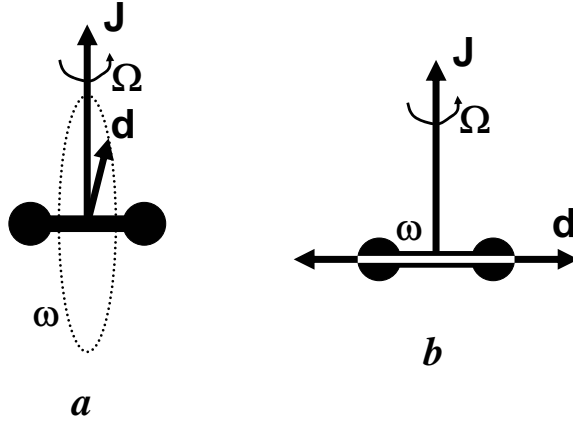


Figure 2. Perpendicular (*a*) and parallel (*b*) type of molecular transition.

$$\langle J' \Lambda = 0 | \hat{d} | J'' \Lambda = 0 \rangle \quad (2)$$

in a straightforward way can be associated with an oscillation with a frequency ω of a transition dipole momentum along the internuclear axis (see Fig. 2 *b*). Unfortunately, this picture alone is not sufficient to understand what will be the spatial distribution of molecular axes or angular momentum of molecules after the molecules absorb the polarized light with a fixed polarization in the laboratory frame. The transition dipole, which follow its own motion with frequency ω , simultaneously rotates together with the molecule with a frequency Ω . In order to understand what will be the angular momentum or molecular axis spatial distribution in the laboratory frame when a molecule absorbs polarized light, one needs to decompose the composite motion of the transition dipole momentum into components fixed in the laboratory frame. Most suitable for this purpose are the cyclic components of the vector. The unit vectors of this reference frame can be written as [3, 16, 17]

$$\mathbf{e}_{+1} = -1/\sqrt{2}(\mathbf{e}_x + i\mathbf{e}_y), \quad (3)$$

$$\mathbf{e}_0 = \mathbf{e}_z, \quad (4)$$

$$\mathbf{e}_{-1} = 1/\sqrt{2}(\mathbf{e}_x - i\mathbf{e}_y). \quad (5)$$

These vectors can easily represent the linear oscillations along the z axis (\mathbf{e}_0) and a circular motion in the clockwise (\mathbf{e}_{-1}), as well as counterclockwise (\mathbf{e}_{+1}) direction in the xy plane [13]. In these coordinates a transition, which corresponds to the transition angular momenta component in a laboratory frame d^{+1} , increases the total angular momentum J of the molecule by 1. This is a so-called R type of the molecular transition and it is associated with the rotation of transition dipole moment in a system of coordinates which is fixed to the total angular momentum of molecule in a counterclockwise direction — in a direction that coincides with a direction of the molecular rotation. The transition dipole moment rotation frequency in this case is $\omega + \Omega$. The transition, which corresponds to the transition dipole momenta d^{-1} component, decreases the angular momentum of the molecule by 1. This is a so-called P type of molecular transition and it is associated with the rotation of the transition dipole moment in a clockwise direction — in a direction which is opposite to the direction of molecular rotation. The transition dipole moment rotation frequency in this case is $\omega - \Omega$. As far as there is a transition dipole moment component in the plane perpendicular to the total angular momentum of the molecule for both cases of molecular transition — parallel as well as perpendicular — both transition types (P and R) exist for both parallel and perpendicular molecular transition [3, 18]. Additionally, for the perpendicular type of molecular transition there is a component of transition dipole moment in a direction perpendicular to the molecular axis. This component of transition dipole can be associated with linear oscillations along the total angular momentum of the molecule. Frequency of these oscillations is ω . This is a so-called Q type of the molecular transition [3, 18]. All three types of molecular transition are shown in Fig. 3.

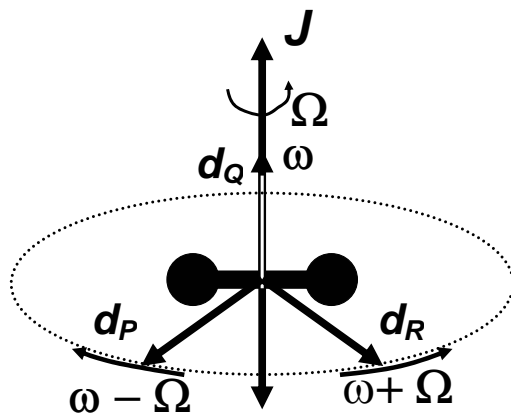


Figure 3. Spatial orientation of transition dipole moment for P , Q and R types of molecular transitions.

This vector model of the transition dipole moment behavior provides a very simple and straightforward way to analyze the kind of spatial distribution of angular momenta or molecular axis that will be created by the absorption of the light of a definite polarization. For example, let us assume that we have light polarized along the z axis and the frequency of the light is equal to the frequency at which the transition dipole oscillates — ω . This light is absorbed by the molecules undergoing Q type transition (transition dipole moment parallel to angular momentum). As far as the classical probability to absorb light by a linear dipole is proportional to $\cos^2 \theta$, where angle θ is an angle between transition dipole moment and an electric vector of the light (see Fig. 4a), it is obvious that in this vector model the spatial distribution $\rho_{cl}(\theta, \varphi)$ of the angular momentum of molecules will be represented by the dumb bell shape probability density function $\rho_{cl}(\theta, \varphi) \sim \cos^2 \theta$, (see Fig. 5a).

Let us now consider the absorption of circularly polarized light. We will describe the handedness of the light in accordance with the definition accepted in optics [19]. It means that if we are looking at the light beam, which is approaching us, and in this beam the electric field vector \mathbf{E} rotates from left to right (clockwise direction) then we will call this light a right-polarized light, but if the electric field vector rotates from right to left (counterclockwise direction) then we will call this light a left-polarized light. Now, for example, a left-polarized light is propagating along the z axis. Its frequency coincides with the frequency $\omega - \Omega$ of the P type transition in a particular molecule (see Fig. 4b). According to the figure, if the angular momentum of the molecule is in the positive direction of the z axis, then the transition dipole moment and the electric field vector of the light rotate in the opposite direction and the molecule is not able to absorb the light. On the contrary, if the angular momentum of the molecules is pointed in the negative direction of the z axis, then the transition dipole moment of the molecule and the light electric field rotate in the same direction with the same angular frequency. This means that such a molecule can absorb the light efficiently. If we are putting the analysis we performed in quantitative terms, then it means that the probability of the molecule to absorb left-hand circularly polarized light that travels in positive direction of z axis in case of P type of molecular transition is proportional to $\rho_{cl}(\theta, \varphi) \sim (1 - \cos \theta)^2/4$, see, Fig. 5b.

Such type of analysis in each particular case of light polarization and type of molecular transition allows to obtain a simple and comprehensive picture, which shows, what kind of angular momentum distribution we can expect if the ensemble of molecules absorbs the light with a specific polarization.

2.2. LIOUVILLE (OPTICAL BLOCH) EQUATIONS

Of course, a vector model described above has strong limitations. It can be applied only in the case of large angular momentum quantum number values. To have a precise quantum mechanical description of light interaction with atoms and molecules, one should use a quantum mechanical description. Usage of monochro-

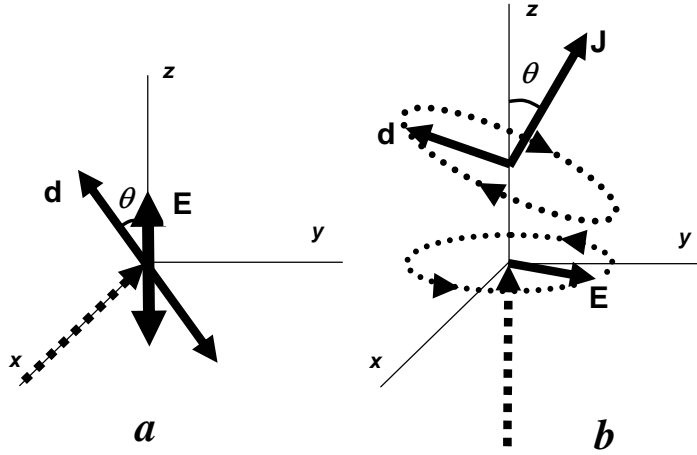


Figure 4. *a* — absorption of lineal polarized light by a *Q* type of molecular transition and *b* — of the left hand circular polarized light by a *P* type of molecular transition.

matic, intense and continuously tunable radiation sources permits a very precise control of atomic and molecular states. To describe this interaction for intense laser radiation, one can use an optical Bloch equation [8, 20]

$$i\hbar \frac{d\rho(t)}{dt} = [H, \rho(t)] + \Gamma \rho(t), \quad (6)$$

where $\rho(t)$ is a density matrix describing population of the levels and coherences created in a system. H is a Hamilton operator, which describes atom or molecule and its interaction with the laser radiation. Finally, Γ is the relaxation matrix, which phenomenologically describes all the relaxation processes in a system. Usually this system of equations is solved in the rotating wave approximation, which eliminates fast oscillations with a frequency of the order of optical transition frequency for the density matrix elements.

For example, in the simplest possible case of two non-degenerated level system interacting with laser radiation, we have the following Liouville equations

$$\dot{\rho}_{11} = \Gamma_1 - \Gamma_1 \rho_{11} + \Gamma_{21} \rho_{22} + \frac{i}{2}(\rho_{12} - \rho_{21})\Omega, \quad (7)$$

$$\dot{\rho}_{12} = -\left(\gamma - i\Delta + \frac{\Gamma_{21} + \Gamma_2 + \Gamma_1}{2}\right) \rho_{12} + \frac{i}{2}(\rho_{11} - \rho_{22})\Omega, \quad (8)$$

$$\dot{\rho}_{22} = -(\Gamma_2 + \Gamma_{21}) \rho_{22} - \frac{i}{2}(\rho_{12} - \rho_{21})\Omega, \quad (9)$$

where Γ_{21} is a spontaneous emission rate from level 2 to level 1 and Γ_i is an additional loss rate from level i , $i = 1, 2$. Excitation is parameterized by a Rabi frequency $\Omega = d_{12}\mathcal{E}/\hbar$, where d_{12} is a dipole operator matrix element between

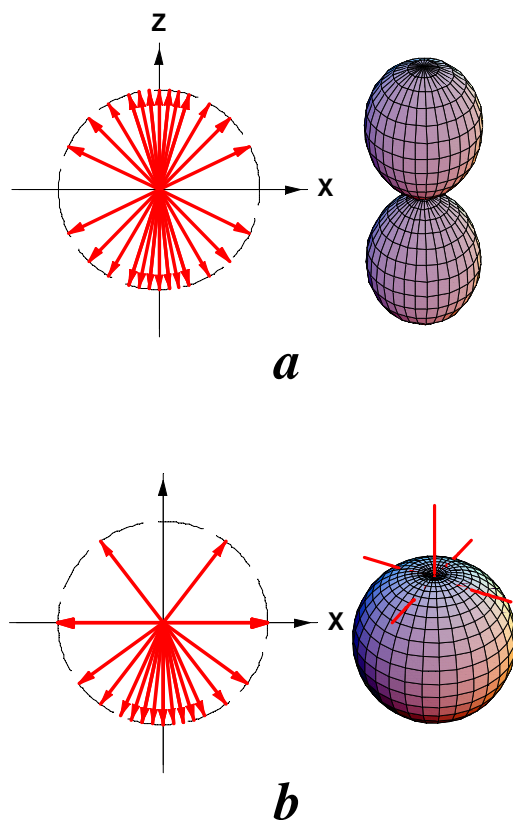


Figure 5. *a* — angular momentum alignment (angular momentum spatial distribution probability density) created by an absorption of linear polarized light on a *Q* type of molecular transition and *b* — angular momentum orientation created by a left-hand polarized light on a *P* type of molecular transition.

states 1 and 2 and \mathcal{E} is an electric field strength of the laser radiation. Parameter Δ describes a detuning of the laser frequency from the exact resonance, γ is equal to the laser radiation spectral line-width, $\rho_{ik} = \rho_{ki}^*$. These equations represent the excitation processes of a two level system with an accuracy which is adequate for most experiments that study collision dynamics or chemical reactions. Even more, molecular systems are often open systems. This means that excited molecules usually decay to very many molecular states and there is a very small chance for a molecule in a spontaneous process to return to the initial level. Consequently, we are arriving at a situation when $\Gamma_{21} = 0$ and even in case of degenerated molecular

states the problem very often can be treated as a set of many independent two level systems. Each system of equations describes an independent pairs of levels from the degenerated two level transition.

This system in many cases can be simplified further. For example, if we have a broad spectral line excitation with a not very intense laser radiation, we have a situation for an open transition when $\gamma \gg \Gamma_i, \Omega$. In practical cases this condition is often fulfilled at excitation with *cw* lasers operating in a multimode regime. If the homogeneous width of spectral transition usually is in the range of 10 MHz, then the laser radiation spectral width broader than 100 MHz usually can be considered as a broad line excitation. In this case we can use a procedure known as adiabatic elimination. It means that we are assuming that optical coherence ρ_{12} decays much faster than the populations of the levels $\rho_{ii}, i = 1, 2$. Then we can find stationary solution for off-diagonal elements for the density matrix and afterwards find a rate equations for populations in this limit. For the two level system we will have

$$\dot{\rho}_{11} = \Gamma_1 - \Gamma_1 \rho_{11} + \Gamma_{21} \rho_{22} - \frac{(2\gamma + \Gamma_1 + \Gamma_2 + \Gamma_{21})\Omega^2}{(2\gamma + \Gamma_1 + \Gamma_2 + \Gamma_{21})^2 + 4\Delta^2} \rho_{11} + \frac{(2\gamma + \Gamma_1 + \Gamma_2 + \Gamma_{21})\Omega^2}{(2\gamma + \Gamma_1 + \Gamma_2 + \Gamma_{21})^2 + 4\Delta^2} \rho_{22}, \quad (10)$$

$$\dot{\rho}_{22} = -(\Gamma_2 + \Gamma_{21}) \rho_{22} + \frac{(2\gamma + \Gamma_1 + \Gamma_2 + \Gamma_{21})\Omega^2}{(2\gamma + \Gamma_1 + \Gamma_2 + \Gamma_{21})^2 + 4\Delta^2} \rho_{11} - \frac{(2\gamma + \Gamma_1 + \Gamma_2 + \Gamma_{21})\Omega^2}{(2\gamma + \Gamma_1 + \Gamma_2 + \Gamma_{21})^2 + 4\Delta^2} \rho_{22}, \quad (11)$$

In these equations that are valid for broad spectral line excitation (large γ) and arbitrary values for all other parameters, one can easily see a simple rate equations if we assume that absorption rate is expressed as

$$\Gamma_{pump} = \frac{(2\gamma + \Gamma_1 + \Gamma_2 + \Gamma_{21})\Omega^2}{(2\gamma + \Gamma_1 + \Gamma_2 + \Gamma_{21})^2 + 4\Delta^2}. \quad (12)$$

If we are interested in a stationary solution of Eqs. (10 and 11), then balance equations that can be obtained from Eqs. (10 and 11) setting right-hand-side of equations equal to zero are valid for any values of parameters and the broad spectral line assumption is not necessary any more. It means that very often for two level system Liouville equations can be replaced with a simple rate equations.

Situation becomes much more complicated if we have a two-step excitation. For example, the first laser excites transition $1 \rightarrow 2$ and the second laser further excites transition $2 \rightarrow 3$. In this case for nondegenerated three level system we will have the following Liouville equations:

For the diagonal elements or the populations of three levels we have

$$\begin{aligned} \dot{\rho}_{11} &= \Gamma_1 - \Gamma_1 \rho_{11} + \Gamma_{21} \rho_{22} + \Gamma_{31} \rho_{33} + \frac{i}{2} (\rho_{12} - \rho_{21}) \Omega_{12}, \\ \dot{\rho}_{22} &= -(\Gamma_2 + \Gamma_{21}) \rho_{22} + \Gamma_{32} \rho_{33} - \end{aligned} \quad (13)$$

$$\frac{i}{2} (\rho_{12} - \rho_{21}) \Omega_{12} + \frac{i}{2} (\rho_{23} - \rho_{32}) \Omega_{23}, \quad (14)$$

$$\dot{\rho}_{33} = -(\Gamma_3 + \Gamma_{31} + \Gamma_{32}) \rho_{33} - \frac{i}{2} (\rho_{23} - \rho_{32}) \Omega_{23}. \quad (15)$$

The density matrix equations for the single-photon coherences are

$$\begin{aligned} \dot{\rho}_{12} = & - \left(\gamma - i\Delta_{12} + \frac{\Gamma_{21} + \Gamma_1 + \Gamma_2}{2} \right) \rho_{12} + \\ & \frac{i}{2} (\rho_{11} - \rho_{22}) \Omega_{12} + \frac{i}{2} \rho_{13} \Omega_{23}, \end{aligned} \quad (16)$$

$$\begin{aligned} \dot{\rho}_{23} = & - \left(\gamma - i\Delta_{23} + \frac{\Gamma_{21} + \Gamma_2 + \Gamma_{31} + \Gamma_{32} + \Gamma_3}{2} \right) \rho_{23} - \\ & \frac{i}{2} \rho_{13} \Omega_{12} + \frac{i}{2} (\rho_{22} - \rho_{33}) \Omega_{23}, \end{aligned} \quad (17)$$

while the equation for the two-photon coherence is

$$\begin{aligned} \dot{\rho}_{13} = & -\frac{1}{2} (-i\Delta_{13} + \Gamma_{31} + \Gamma_{32} + \Gamma_1 + \Gamma_3) \rho_{13} - \\ & \frac{i}{2} \rho_{23} \Omega_{12} + \frac{i}{2} \rho_{12} \Omega_{23}. \end{aligned} \quad (18)$$

In these equations all the notations are similar to the notations used for the two level system.

The procedure of adiabatic elimination in this case leads to rather complicated equations for diagonal elements of the density matrix, which in a general case can not be reduced to simple rate equations for populations. To examine the essential characteristics of the equations for populations we shall make a number of simplifying assumptions. First, let us consider an exact resonance

$$\Delta_{ij} = 0. \quad (19)$$

Next, we neglect all spontaneous emission between states 1, 2 and 3. (Such terms are essential when one deals with a closed system, but can often be neglected for such an open system as most of molecules.) We assume that the remaining relaxation rates, to other levels, are all equal:

$$\Gamma_{ij} = 0, \quad \Gamma_j = \Gamma. \quad (20)$$

Finally, we take the two Rabi frequencies to be equal,

$$\Omega_{ij} = \Omega. \quad (21)$$

With these assumptions we have the following rate equations for populations in an assumption of broad spectral line excitation

$$\dot{\rho}_{11} = \Gamma(1 - \rho_{11}) - \frac{\Gamma\Omega^2(\rho_{11} - \rho_{22})}{2\Gamma(\gamma + \Gamma) + \Omega^2} + \frac{\Omega^4(\rho_{11} - \rho_{33})}{4(\gamma + \Gamma)[2\Gamma(\gamma + \Gamma) + \Omega^2]}, \quad (22)$$

$$\dot{\rho}_{22} = -\Gamma\rho_{22} + \frac{\Gamma\Omega^2(\rho_{11} - \rho_{22})}{2\Gamma(\gamma + \Gamma) + \Omega^2} + \frac{\Gamma\Omega^2(\rho_{33} - \rho_{22})}{2\Gamma(\gamma + \Gamma) + \Omega^2}, \quad (23)$$

$$\dot{\rho}_{33} = -\Gamma\rho_{33} - \frac{\Gamma\Omega^2(\rho_{33} - \rho_{22})}{2\Gamma(\gamma + \Gamma) + \Omega^2} + \frac{\Omega^4(\rho_{11} - \rho_{33})}{4(\gamma + \Gamma)[2\Gamma(\gamma + \Gamma) + \Omega^2]}. \quad (24)$$

from where one and two photon absorption rates can be defined as

$$\Gamma_{pump}(1) = \frac{\Omega^2\Gamma}{2\Gamma(\gamma + \Gamma) + \Omega^2}, \quad (25)$$

$$\Gamma_{pump}(2) = \frac{\Omega^4}{4(\gamma + \Gamma)[2\Gamma(\gamma + \Gamma) + \Omega^2]}. \quad (26)$$

If, as before, we are interested only in the steady state solution (steady state populations) for three levels, then the obtained equations are valid for arbitrary values of all the parameters and the assumption of broad spectral line (large γ) is not needed.

In these equations we can clearly see the two photon transition probabilities that directly connect levels 1 and 3 and are proportional to the fourth power of Rabi frequency. These equations in the limit of weak excitation (small Ω) lead to the "phenomenological" rate equations, which do not take into account two photon transitions

$$\dot{\rho}_{11} = \Gamma(1 - \rho_{11}) - \frac{\Omega^2(\rho_{11} - \rho_{22})}{2(\gamma + \Gamma)}, \quad (27)$$

$$\dot{\rho}_{22} = -\Gamma\rho_{22} + \frac{\Omega^2(\rho_{11} - \rho_{22})}{2(\gamma + \Gamma)} + \frac{\Omega^2(\rho_{33} - \rho_{22})}{2(\gamma + \Gamma)}, \quad (28)$$

$$\dot{\rho}_{33} = -\Gamma\rho_{33} - \frac{\Omega^2(\rho_{33} - \rho_{22})}{2(\gamma + \Gamma)}. \quad (29)$$

We see that, taking into account assumptions made with respect to the relaxation rates and other parameters, we basically have arrived at the same absorption rate that we had for a two level system, compare to Eq. (12). It is interesting to note the ratio between two-photon transition rate and one-photon transition rate. This ratio is

$$\frac{\Gamma_{pump}(2)}{\Gamma_{pump}(1)} = \frac{\Omega^2}{4\Gamma(\gamma + \Gamma)}, \quad (30)$$

which means that the transition rate for two photon transitions is negligible for weak excitation, but can play a dominant role for strong laser radiation and cannot be neglected.

To illustrate the method described above, let us consider now one particular example (see Fig. 6). The diatomic molecule, for example Na_2 , is excited in two steps by two weak linear polarized lasers, which are at an exact resonance ($\Delta = 0$) — first one with the first molecular transition, but the second one with the second molecular transition. In the first case lasers are polarized parallel to each other.

Angular momenta of the molecular states involved in the transition are $J'' = 7 \rightarrow J'_1 = 8 \rightarrow J'_2 = 9$. As a result we have molecular axis distribution in the second excited state as depicted in the Fig. 6a. The z axis in this figure is directed along the direction of polarization of both lasers. As we see, molecular axes are very strongly aligned along the direction of quantization axis (direction of polarization of a laser beams).

On the contrary, if we have lasers polarized in perpendicular directions to each other, we point the z -axis in the direction of polarization of second laser and consider molecular transitions in a sequence $J'' = 7 \rightarrow J'_1 = 8 \rightarrow J'_2 = 8$, then we have molecular axes distribution in the second excited state as shown in Fig. 6b. Now molecular axes are very strongly aligned in the plane that is perpendicular to the axis of quantization. This example demonstrates, how efficiently we can manipulate the molecular axes distribution just by varying angular momentum of the states excited by laser beams and mutual polarization of lasers.

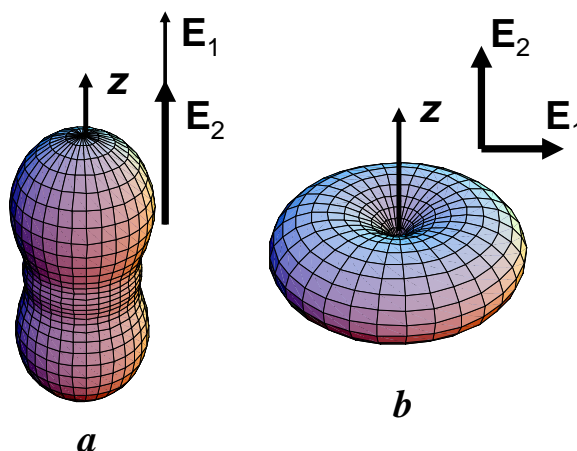


Figure 6. The probability distribution of molecular axes for two step laser excitation of diatomic molecules. For case *a* we have angular momentum quantum number sequence 7-8-9 in molecular transitions, but for case *b* we have 7-8-8 sequence. Mutual laser polarization for both cases is shown in the figure.

3. Rate equations for degenerate levels

Let us analyze further to what consequences assumption of spectrally broad laser excitation leads. We shall assume that we have degenerate ground and excited state of optical transition. For example, it can be an optical transition between two molecular states that consists of a large number of degenerate magnetic (Zeeman) sublevels. It means that this large width of laser line will prevent the formation of the optical coherences between pairs of magnetic sublevels, in which one sublevel

belongs to the ground state and another to the excited state – optical coherences. At the same time there is no reason why, with the spectrally broad radiation, coherences between pairs of magnetic sublevels for which both sublevels belong either to the ground or to the excited state could not be created. To analyze these Zeeman coherences, the density matrix equations for degenerated two level system for a broad spectral line excitation can be used [3, 12]

$$\begin{aligned}
\dot{f}_{M_e M'_e} &= \Gamma_p \sum_{M_g M'_g} \langle M_e | \mathbf{E}^* \mathbf{d} | M_g \rangle \langle M'_e | \mathbf{E}^* \mathbf{d} | M'_g \rangle^* \varphi_{M_g M'_g} - \\
&\quad \left(\frac{\Gamma_p}{2} + i\omega_S \right) \sum_{M''_e M_g} \langle M_e | \mathbf{E}^* \mathbf{d} | M_g \rangle \langle M''_e | \mathbf{E}^* \mathbf{d} | M_g \rangle^* f_{M''_e M'_e} - \\
&\quad \left(\frac{\Gamma_p}{2} - i\omega_S \right) \sum_{M''_e M_g} \langle M''_e | \mathbf{E}^* \mathbf{d} | M_g \rangle \langle M'_e | \mathbf{E}^* \mathbf{d} | M_g \rangle^* f_{M_e M''_e} - \\
&\quad \Gamma f_{M_e M'_e} - i\omega_{M_e M'_e} f_{M_e M'_e} \tag{31} \\
\dot{\varphi}_{M_g M'_g} &= - \left(\frac{\Gamma_p}{2} + i\omega_S \right) \sum_{M''_g M_e} \langle M_g | \mathbf{E}^* \mathbf{d} | M_e \rangle \langle M''_g | \mathbf{E}^* \mathbf{d} | M_e \rangle^* \varphi_{M''_g M'_g} - \\
&\quad \left(\frac{\Gamma_p}{2} - i\omega_S \right) \sum_{M''_g M_e} \langle M''_g | \mathbf{E}^* \mathbf{d} | M_e \rangle \langle M'_g | \mathbf{E}^* \mathbf{d} | M_e \rangle^* \varphi_{M_g M''_g} + \\
&\quad \Gamma_p \sum_{M_e M'_e} \langle M_g | \mathbf{E}^* \mathbf{d} | M_e \rangle \langle M'_g | \mathbf{E}^* \mathbf{d} | M'_e \rangle^* f_{M_e M'_e} - \gamma \varphi_{M_g M'_g} - \\
&\quad i\omega_{M_g M'_g} \varphi_{M_g M'_g} + \sum_{M_e M'_e} \Gamma_{M_g M'_g}^{M_e M'_e} f_{M_e M'_e} + \lambda \delta_{M_g M'_g} \tag{32}
\end{aligned}$$

where by $f_{M_e M'_e}$ and $\varphi_{M_g M'_g}$ are denoted the density matrices of an excited and ground state level respectively. The first term on the right-hand side of Eq.(31) describes the absorption of light at the rate Γ_p . The transition matrix elements of the form $\langle M_e | \mathbf{E}^* \mathbf{d} | M_g \rangle$ account for the conservation of angular momentum during photon absorption with \mathbf{E} being the light polarization vector. The second and the third terms describe the stimulated emission of the light and the dynamic Stark shift ω_S . The fourth term characterizes the relaxation of the density matrix $f_{M_e M'_e}$ with a rate constant Γ . Finally, the fifth term describes the Zeeman splitting of the magnetic sublevels M_e and M'_e by a value of $\omega_{M_e M'_e} = (E_{M_e} - E_{M'_e})/\hbar$.

The first and the second terms on the right-hand side of Eq.(32) describe a light absorption and the dynamic Stark shift, the third term — the stimulated light emission, the fourth term — the relaxation processes in the ground state, the fifth term — the Zeeman interaction, the sixth term — the repopulation by spontaneous transitions at a rate $\Gamma_{M_g M'_g}^{M_e M'_e}$, and the seventh term — the relaxation of the density matrix of the ground state atoms interacting with the gas in a cell, not influenced by the radiation.

The matrix element of electric dipole transition $\langle M_e | \mathbf{E}^* \mathbf{d} | M_g \rangle$ is expanded as [3, 16, 17]

$$\langle M_e | \mathbf{E}^* \mathbf{d} | M_g \rangle = \sum_q (E^q)^* \langle M_e | d^q | M_g \rangle, \quad (33)$$

where the superscript q denotes the cyclic components of the respective vectors. The matrix element at the right-hand side of equation (33) are further expanded, applying the Wigner–Eckart theorem, as [3, 16, 17]

$$\langle M_e | d^q | M_g \rangle = \frac{1}{\sqrt{2F_e + 1}} C_{J_g M_g 1 q}^{J_e M_e} (F_e \| d \| F_g), \quad (34)$$

where $(J_e \| d \| J_g)$ is the reduced matrix element. Under conditions of stationary excitation the system of equations (31) and (32) becomes a system of linear equations for the ground and excited state density matrix elements. The coefficients of this system are calculated using angular momentum algebra and the formulas presented above. For further details see, for example [3].

Solution of this equation allows to calculate spatial distribution and its evolution in time for angular part of probability density, which in case of atoms means angular distribution of valence electron but in case of diatomic molecules — the spatial distribution of molecular axis. This is an important information, if the stereo effects for different interactions are under the study. Hence, for example, if we know the density matrix of the excited state of diatomic molecule, then the molecular axes distribution can simply be calculated as [15]

$$\rho_{\alpha x}(\theta, \varphi) = \sum_{M_1 M_2} f_{M_1 M_2} Y_{J M_1}(\theta, \varphi) Y_{J M_2}^*(\theta, \varphi). \quad (35)$$

If one is interested in a spatial distribution of angular momentum created by laser radiation, then there is a method how to make a transition from quantum density matrix to the continuous angular momentum spatial distribution probability density. As it is shown in [21], a classical probability density $\rho_{cl}(\theta, \varphi)$ for angular momentum spatial distribution can be connected to the density matrix elements $f_{MM'}$. At the $J \rightarrow \infty$ limit these elements can be considered as coefficients of the Fourier expansion of a classical probability density $\rho_{cl}(\theta, \varphi)$

$$\rho_J(\theta, \varphi) = \sum_{\epsilon=-\infty}^{\infty} e^{i\epsilon\varphi} f_{M+\frac{\epsilon}{2}, M-\frac{\epsilon}{2}}; \quad \cos\theta = \frac{2M}{2J+1}. \quad (36)$$

The last equation is not restricted to the case when we have a coherent superposition of two M states belonging to the same J . If they belong to different J states, all we need to do is replace J with $(J_1 + J_2)/2$. The inverse of (36) can be written as

$$f_{M+\frac{\epsilon}{2}, M-\frac{\epsilon}{2}} = \frac{1}{2\pi} \int_0^{2\pi} e^{-i\epsilon\varphi} \rho_{cl}(\theta, \varphi) d\varphi. \quad (37)$$

In practice, we almost always have the situation when for those $f_{M+\frac{\varepsilon}{2}, M-\frac{\varepsilon}{2}}$ that differ from zero, values of ε are small in comparison to the interval of all allowed M values. For most cases of practical interest it makes the calculation of (36) rather simple.

4. Influence of external fields

The action of the external fields like electric or magnetic can be taken into account in a very general way. External fields, as a rule, lift the degeneracy of different magnetic sublevels of the angular momentum state. It means that in the external field magnetic sublevels are split and cause appearance of the nonzero Zeeman frequencies $\omega_{M_e M'_e} = (E_{M_e} - E_{M'_e})/\hbar$. For different molecules in different (electric or magnetic) fields pattern of magnetic sublevel splitting can be very different. It means that Zeeman frequencies $\omega_{M_e M'_e}$ can have different dependence on M_e , M'_e for different cases. The simplest case is the linear Zeeman effect, when in the magnetic field each magnetic sublevel obtains additional energy, which is directly proportional to the magnetic field strength and magnetic quantum number. The coefficient of proportionality is the Bohr magneton μ_B multiplied by the Lande factor g

$$E_M = g\mu_B B M. \quad (38)$$

As a result, Zeeman frequencies are simply $\omega_{M_e M'_e} = g\mu_B B \Delta M/\hbar$, where $\Delta M = M - M'$. In terms of the vector model described above, this means that the linear Zeeman effect causes precession of the angular momentum probability distribution around the magnetic field with Larmor frequency $\omega_{Larmor} = g\mu_B B/\hbar$. Shape of probability density during this precession is preserved [15]. However, in many cases Zeeman effect deviates from a simple linear behavior and then the influence of the external field on the polarization of molecules created by the laser field can be a sensitive probe of this nonlinearity of Zeeman effect. As it was shown, for example, for Te_2 in [22] and [23], the nonlinearity of the Zeeman effect can cause a symmetry breaking of the angular momentum spatial distribution, which exhibits itself as an appearance of the orientation of angular momentum in the initially aligned ensemble and appearance of the circularly polarized laser induced fluorescence after linear polarized laser excitation, as a consequence. Observation of such type of effects allows to study the reasons for nonlinearity of the Zeeman effect and to determine such molecular constants as the rate of magnetic predissociation and state mixing matrix elements in external fields. In this particular case a rather strong circularity (up to 5%) was observed at a magnetic field strength of 0.4 T (see Fig. 7)

In the case of an electric field, situation can be even more peculiar. In most cases Stark effect in molecules is in principle nonlinear (quadratic) over the electric field strength \mathcal{E} and magnetic quantum number M . This allows to exploit this intrinsic nonlinearity and to manipulate angular momentum spatial distribution of

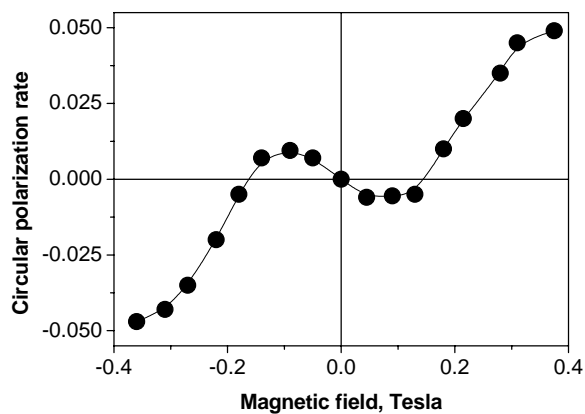


Figure 7. Circular polarization rate created by an alignment to orientation conversion in laser excited fluorescence of the Te_2 molecule due to magnetic intramolecular interactions and magnetic predissociation.

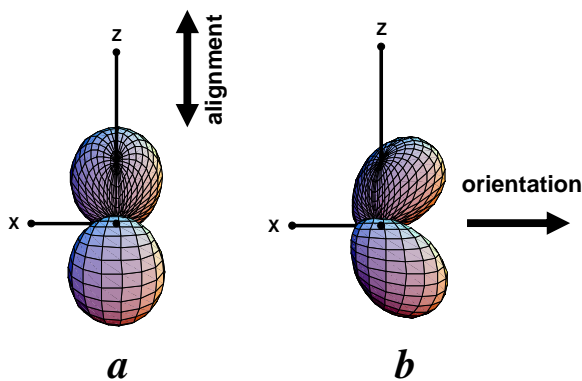


Figure 8. The angular momentum probability distribution of diatomic molecule in absence of an electric field — case *a* and when electric field is applied along the z axis — case *b*.

molecules. Let us consider one example. In Fig. 8 angular momenta spatial distribution are shown for two cases. In case *a* we have initially aligned molecules. This alignment is created by a linearly polarized laser radiation in Q type of molecular transition. Laser is polarized in yz plane at an angle $\pi/4$ with respect to z axis. Molecules are aligned along the laser polarization vector. If now an electric field is applied along z axis angular momenta distribution is changed in such a way that more angular momenta are pointed in the negative direction of x axis than in the

positive direction. As a result, we have transverse (perpendicular to the axis of quantization) orientation of angular momenta of molecules. For more details, see [15].

This alignment to orientation conversion can be exploited for practical purposes. In molecular beams alignment of angular momentum of molecules due to collisions during the beam formation usually occurs almost automatically [24]. If we apply an electric field in the direction of $\pi/4$ to the beam direction, this alignment can be efficiently converted into orientation. Choosing appropriate region length along the beam direction in which field is applied and field strength one can orient molecules in a selected rotational state and even for a selected isotopomer of the molecule. For details, see [25].

When speaking about nonlinear Zeeman or Stark effects in molecules as well as in atoms, we should keep in mind that usually these nonlinearities are caused by mixing in the external field of the different molecular states — be that rotational states of the molecules or other close lying states like, for example, Lambda doublet components in the Π states of the diatomic molecules. This state mixing does not only cause nonlinear magnetic sublevel splitting but also modifies state wave functions between which light causes transitions. It means that the matrix elements of a type $\langle M_e | \mathbf{E} \cdot \mathbf{d} | M_g \rangle$ do not describe any more transition probabilities between states with well defined angular momentum J but between states the wave function of which, in general case, can be represented as

$$|\chi M_g\rangle = \sum_{J_i} c_{J_i} |J_i M_g\rangle. \quad (39)$$

As it was shown in [26], this leads to the substantial modification of the transition probabilities between molecular states and it can happen that transitions that are strictly forbidden in absence of the external field, in presence of the field become to be allowed and exhibit high probability.

5. Conclusions

In this paper it was very briefly demonstrated that the laser radiation in combination with external fields can be a powerful tool to prepare molecules in specific quantum state that can be characterized with a well pronounced spatial anisotropy of molecular axes (chemical bonds) and angular momentum. These states in past have been exploited in studies of molecular properties including dynamics of chemical reactions, but it seems that full capacity of this method still needs to be explored.

Acknowledgements

I am very thankful to Dr. Bruce W. Shore for informal and unhurried discussions about the issues touched in this paper, that I personally enjoyed immensely.

References

1. W. Hanle, Über magnetische Beeinflussung der Polarisation der Resonanzfluoreszenz, *Z. Phys.* **30**, p. 93 – 105, (1924); English translation in ref. 2.
2. *The Hanle Effect and Level-Crossing Spectroscopy*, Edited by G. Morruzi and F. Strumia (Plenum Press, New York, London, 1991), 371 pp.
3. M. Auzinsh and R. Ferber, *Optical Polarization of Molecules* (Cambridge University Press, Cambridge, 1995), 306 pp.
4. A. Kastler, Quelques suggestion conceant la production optique et la detection optique d'une inegelite de population des niveaux, *J. Phys. Radium*, **11**, p. 225 – 265, (1950).
5. Brossel, J., A. Kastler, and J. Winter, Optical method of creating an inequality of population between Zeeman sub-levels of atomic ground states. *J. Phys. Radium*, **13**, p. 668-669, (1952).
6. W.B. Hawkin, R.H. Dicke, The Polarization of Sodium Atoms, *Phys. Rev.*, **91**, p. 1008 – 1009, (1953).
7. G. Alzetta, A. Gozzini, L. Moi, and G. Orrioli, An Experimental Method for the Observation of R.F. Transitions and Laser Bear Resonance in Oriented Na Vapour, *Novo Cimento*, **36**, p. 5 – 20, (1976).
8. E. Arimondo, Coherent population trapping in laser spectroscopy, *Progr. Opt.* **35**, p. 257 – 354, (1996).
9. U. Fano, Description of States in Quantum Mechanics by Density Matrix and Operator Techniques, *Rev. Mod. Phys.*, **29**, p. 74 – 93, (1957).
10. C. Cohen-Tannoudji, Theorie quantique du cycle de pompage optique. Verification experimentale des nouveaux effets prevus (1-e partie), *Ann. De Phys.* **7**, p. 423 – 461, (1962); C. Cohen-Tannoudji, (2-e partie), *Ann. De Phys.* **7**, p. 469 – 504, (1962).
11. Ducloy, M., Nonlinear Effects in Optical Pumping of Atoms by a High-Intensity Multimode Gas Laser. General Theory. *Phys. Rev. A*, **8** (4): p. 1844 – 1859, (1973).
12. Auzinsh, M.P. and R.S. Ferber, Optical-Pumping of Diatomic Molecules in the Electronic Ground State — Classical and Quantum Approaches. *Phys. Rev. A*, **43** (5): p. 2374 – 2386, (1991).
13. Auzinsh, M., The evolution and revival structure of angular momentum quantum wave packets. *Canadian Journal of Physics*, **77** (7): p. 491 – 503, (1999).
14. Rochester, S.M. and D. Budker, Atomic polarization visualized. *Am. J. Phys.*, **69** (4): p. 450 – 454, (2001).
15. Auzinsh, M., Angular momenta dynamics in magnetic and electric field: Classical and quantum approach. *Canadian Journal of Physics*, **75** (12): p. 853-872, (1997).
16. R.N. Zare, *Angular momentum* (J. Wiley & sons, New York, 1988), 280 pp.
17. D.A. Varshalovich, A.N. Moskalev, V.K. Khersonskii, *Quantum theory of angular momenta* (World Scientific, Singapore, 1988), 514 pp.
18. D.A Case, G.M. McClelland, and D.R Herschbach, Angular Momentum Polarization in Molecular Collisions: Classical and quantum theory for measurements using resonance fluorescence, *Mol. Phys.*, **35**, 541 – 573, (1978).
19. M. Born, E. Wolf, *Principles of Optics* (Pergamon Press, Oxford, London, Edinburgh, New York, Paris, Frankfurt, 1968), 566 pp.
20. B.W. Shore, *The Theory of Coherent Atomic Excitation*, (John Wiley & Sons, New York, Chichester, Brisbane, Toronto, Singapore, 1991), vol. 1 and vol. 2, 1735 pp.
21. Nasyrov, K.A., Wigner representation of rotational motion. *J. Phys. A: Math. Gen.*, **32**, p. 6663 – 6678 (1999).
22. Klincare, I.P., M.Y. Tamanis, A.V. Stolyarov, M.P. Auzinsh, and R.S. Ferber, Alignment-Orientation Conversion by Quadratic Zeeman-Effect — Analysis and Observation for Te₂, *J. Chem. Phys.*, **99** (8): p. 5748 – 5753, (1993).
23. Auzinsh, M., A.V. Stolyarov, M. Tamanis, and R. Ferber, Magnetic field induced alignment - orientation conversion: Non-linear energy shift and predissociation in Te₂ B 1_u state, *J. Chem. Phys.*, **105** p. 37 – 49 (1996).

24. Aquilanti, V., D. Ascenzi, M.d. Castro, Vitores, F. Pirani, and D. Cappelletti, A quantum mechanical view of molecular alignment and cooling in seeded supersonic expansions. *J. Chem. Phys.* **111** (6), p. 2620 - 2632, (1999).
25. Auzinsh, M.P. and R.S. Ferber, J-Selective Stark Orientation of Molecular Rotation in a Beam., *Phys. Rev. Lett.*, **69** (24): p. 3463 - 3466, (1992).
26. Tamanis, M., M. Auzinsh, I. Klincare, O. Nikolayeva, A.V. Stolyarov, and R. Ferber, NaK D 1^{II} electric dipole moment measurement by Stark level crossing and e-f mixing spectroscopy., *J. Chem. Phys.* **106** (6), p. 2195 - 2204 (1997).